QCD corrections to Υ production via color-octet states at the Tevatron and LHC

Bin Gong,[1,2,3] Jian-Xiong Wang,[1,3] and Hong-Fei Zhang[1,3]

[1]*Institute of High Energy Physics, CAS, P.O. Box 918(4), Beijing, 100049, China*
[2]*Institute of Theoretical Physics, CAS, P.O. Box 2735, Beijing, 100190, China*
[3]*Theoretical Physics Center for Science Facilities, CAS, Beijing, 100049, China*

(Received 21 September 2010; revised manuscript received 19 March 2011; published 9 June 2011)

The next-to-leading order QCD corrections to Υ production via S-wave color-octet states $\Upsilon[^1S_0^{(8)}, {}^3S_1^{(8)}]$ at the Tevatron and LHC is calculated. The K factors of total cross section (ratio of next-to-leading order to leading order) are 1.313 and 1.379 for $\Upsilon[^1S_0^{(8)}]$ and $\Upsilon[^3S_1^{(8)}]$ at the Tevatron, while at the LHC they are 1.044 and 1.182, respectively. By fitting the experimental data from the CDF and D0, the matrix elements for S-wave color-octet states are obtained. And new predictions for $\Upsilon(1S)$ production are presented. The prediction for the polarization of inclusive Υ contains large uncertainty rising from the polarization of $\Upsilon(1S)$ from feed-down of χ_b. The production of $\Upsilon(3S)$ at the hadron colliders is also studied to avoid the large uncertainty mentioned above. To further clarify the situation, new measurements on the production and polarization for direct $\Upsilon(1S)$ and $\Upsilon(3S)$ are expected.

DOI: 10.1103/PhysRevD.83.114021 PACS numbers: 12.38.Bx, 13.25.Gv, 13.60.Le

I. INTRODUCTION

For heavy quarkonium production and decay, a naive perturbative QCD and nonrelativistic factorization treatment is applied straightforwardly. It is called the color-singlet mechanism (CSM). To describe the huge discrepancy of the high-p_t J/ψ production between the theoretical prediction based on CSM and the experimental measurement at the Tevatron, the color-octet (CO) mechanism [1] was proposed based on the nonrelativistic QCD (NRQCD) [2]. In applications, J/ψ or Υ related productions or decays attract much attention for two reasons, theoretically charm and bottom quarks are thought to be heavy enough, so that charmonium and bottomonium can be treated within the NRQCD framework; experimentally there is a very clear signal to detect J/ψ and Υ. The key point is that the color-octet mechanism depends on nonperturbative universal NRQCD matrix elements, which are obtained by fitting the data. Therefore, various efforts have been made to confirm this mechanism, or to fix the magnitudes of the universal NRQCD matrix elements. Although it seems that the theoretical calculations qualitatively agree with the experimental data, there are still difficulties remaining. A review of the situation can be found in Refs. [3,4].

To explain the experimental measurements [5,6] of J/ψ production at the B factories, a series of calculations [7,8] in the CSM reveal that the next-to-leading order (NLO) QCD corrections give the main contribution to the related processes. Together with the relativistic correction [9], it seems that most experimental data for J/ψ production at the B factories could be understood. Recent studies show that the NLO QCD correction also plays an important role in J/ψ production at RHIC [10] and the hadroproduction of χ_c [11]. For the J/ψ photoproduction, the p_t and z distributions can be described by the NLO calculations in CSM [12] by choosing a small renormalization scale, but recent NLO calculations in CSM [13] show that the p_t distributions of the production and polarization for J/ψ can not be well described by choosing proper renormalization scale. Although the complete calculation at NLO in CO mechanism [14] can account for the experimental measurements on the p_t distribution, the polarization was not studied in the work. To further study the heavy quarkonium production mechanism, there are many other efforts made, such as NLO QCD corrections to J/ψ production associated with photon [15], QED contributions in J/ψ hadroproduction [16], inclusive J/ψ production from Υ decay [17], double heavy quarkonium hadroproduction [18], and NLO QCD corrections to J/ψ production from Z decay [19].

For the polarized heavy quarkonium hadroproduction, the leading order (LO) NRQCD prediction gives a sizable transverse polarization for J/ψ production at high p_t at the Tevatron while the experimental measurement [20] gives a slight longitudinal polarized result. The discrepancy was also found in Υ production. In a recent paper [21], the measurement on polarization of Υ production at the Tevatron is presented and the NRQCD prediction [22] does not coincide with it. Within the NRQCD framework, calculating the higher order corrections is thought to be an important way towards the solution of such puzzles. Recently, NLO QCD corrections to J/ψ and Υ hadroproduction have been calculated [23–27], and the results show that the NLO QCD corrections give significant enhancement to both total cross section and momentum distribution for the color-singlet channel. This would reduce the contribution of color-octet channel in the production. Also, it is found in Ref. [24] that the polarizations for J/ψ and Υ hadroproduction via the color-singlet channel would change drastically from transverse polarization dominant at LO into longitudinal polarization dominant in the whole range of the transverse momentum p_t at NLO. It seems that

these results open a door to the solution of the problem. But things do not always go as expected. The NLO QCD corrections to the J/ψ production via S-wave color-octet states were studied in our previous work [28]. It was found that the effect of NLO QCD corrections is small and the discrepancy holds on. For the color-singlet part, the partial next-to-next-to-leading order calculations for Υ and J/ψ hadroproduction show that the uncertainty from higher order QCD corrections [29] is quite large, therefore no definite conclusion can be made. As we know, the contribution from the color-octet states is smaller in Υ production than that in J/ψ production, thus things may be different. In this paper, we present our calculation on NLO QCD corrections to Υ hadroproduction via S-wave color-octet states. New matrix elements are fitted and new predictions for the polarization status are presented.

This paper is organized as follows. In Sec. II, we give the LO cross section for the processes via color-octet transition. The calculation of NLO QCD corrections are described in Sec. III. In Sec. IV, we present the formula in final integration to obtain the transverse momentum distribution of Υ production. Sec. V. is devoted to the description about the calculation of Υ polarization. The numerical results are presented in Sec. VI. In Sec. VII, $\Upsilon(3S)$ is studied, while the summary and discussion are given in Sec. VIII. In the Appendices, several details of the calculation are presented.

II. THE LO CROSS SECTION

According to the NRQCD factorization formalism, the cross section for direct Υ production in hadron-hadron collision is expressed as

$$\sigma[pp \to \Upsilon + X] = \sum_{i,j,k,n} \int dx_1 dx_2 G_{i/p} G_{j/p} \times \hat{\sigma}[i + j \to (b\bar{b})_n + k] \langle \mathcal{O}_n^{\Upsilon} \rangle, \quad (1)$$

where p is either a proton or an antiproton, the indices i, j, k run over all the partonic species and n denotes the color, spin and angular momentum states of the intermediate $b\bar{b}$ pair. The short-distance contribution $\hat{\sigma}$ can be perturbatively calculated order by order in α_s. The hadronic matrix elements $\langle \mathcal{O}_n^{\Upsilon} \rangle$ are related to the hadronization from the state $(b\bar{b})_n$ into Υ which are fully governed by the nonperturbative QCD effects. In the following, $\hat{\sigma}$ represents the corresponding partonic cross section.

At LO, there are three partonic processes via CO transition:

$$g(p_1) + g(p_2) \to \Upsilon[^1S_0^{(8)}, {}^3S_1^{(8)}](p_3) + g(p_4), \quad \text{(L1)}$$

$$g(p_1) + q(p_2) \to \Upsilon[^1S_0^{(8)}, {}^3S_1^{(8)}](p_3) + q(p_4), \quad \text{(L2)}$$

$$q(p_1) + \bar{q}(p_2) \to \Upsilon[^1S_0^{(8)}, {}^3S_1^{(8)}](p_3) + g(p_4). \quad \text{(L3)}$$

where q represents a sum over all possible light quarks or antiquarks: u, d, s, c, $\bar{u}$, $\bar{d}$, $\bar{s}$ and $\bar{c}$. In our calculation of Υ production, we take charm quark as light quark as an approximation. Typical Feynman diagrams for these three processes are shown in Fig. 1. And the partonic differential cross sections in $n = 4 - 2\epsilon$ dimension for LO processes can be obtained as

$$\begin{aligned}
\frac{d\hat{\sigma}^B(q\bar{q} \to \Upsilon[^3S_1^{(8)}]g)}{d\hat{t}} &= \frac{\pi^2\alpha_s^3\langle \mathcal{O}_8^{\Upsilon}(^3S_1)\rangle[(\hat{t}-1)^2 + (\hat{u}-1)^2][4\hat{t}^2 - \hat{t}\,\hat{u} + 4\hat{u}^2]}{324 m_b^5 \hat{s}^2(\hat{s}-1)^2\hat{t}\,\hat{u}} + \mathcal{O}(\epsilon),\\
\frac{d\hat{\sigma}^B(gq \to \Upsilon[^3S_1^{(8)}]q)}{d\hat{t}} &= \frac{-\pi^2\alpha_s^3\langle \mathcal{O}_8^{\Upsilon}(^3S_1)\rangle[(\hat{s}-1)^2 + (\hat{u}-1)^2][4\hat{s}^2 - \hat{s}\,\hat{u} + 4\hat{u}^2]}{864 m_b^5 \hat{s}^3(\hat{t}-1)^2\hat{u}} + \mathcal{O}(\epsilon),\\
\frac{d\hat{\sigma}^B(gg \to \Upsilon[^3S_1^{(8)}]g)}{d\hat{t}} &= \frac{\pi^2\alpha_s^3\langle \mathcal{O}_8^{\Upsilon}(^3S_1)\rangle[(\hat{s}^2-1)^2 + (\hat{t}^2-1)^2 + (\hat{u}^2-1)^2 - 6\hat{s}\,\hat{t}\,\hat{u} - 2][19 - 27(\hat{s}\,\hat{t} + \hat{t}\,\hat{u} + \hat{u}\,\hat{s})]}{1152 m_b^5 \hat{s}^2(\hat{t}-1)^2(\hat{u}-1)^2(\hat{s}-1)^2} + \mathcal{O}(\epsilon),\\
\frac{d\hat{\sigma}^B(q\bar{q} \to \Upsilon[^1S_0^{(8)}]g)}{d\hat{t}} &= \frac{5\pi^2\alpha_s^3\langle \mathcal{O}_8^{\Upsilon}(^1S_0)\rangle[\hat{t}^2 + \hat{u}^2]}{216 m_b^5 \hat{s}^3(\hat{s}-1)^2} + \mathcal{O}(\epsilon),\\
\frac{d\hat{\sigma}^B(gq \to \Upsilon[^1S_0^{(8)}]q)}{d\hat{t}} &= \frac{-5\pi^2\alpha_s^3\langle \mathcal{O}_8^{\Upsilon}(^1S_0)\rangle[\hat{s}^2 + \hat{u}^2]}{576 m_b^5 \hat{s}^2\hat{t}(\hat{t}-1)^2} + \mathcal{O}(\epsilon),\\
\frac{d\hat{\sigma}^B(gg \to \Upsilon[^1S_0^{(8)}]g)}{d\hat{t}} &= \frac{5\pi^2\alpha_s^3\langle \mathcal{O}_8^{\Upsilon}(^1S_0)\rangle[\hat{s}^2\hat{t}^2 + \hat{s}^2\hat{u}^2 + \hat{t}^2\hat{u}^2 + \hat{s}\,\hat{t}\,\hat{u}][\hat{s}^4 + \hat{t}^4 + \hat{u}^4 + 1]}{256 m_b^5 \hat{s}^3\hat{t}\,\hat{u}(\hat{t}-1)^2(\hat{u}-1)^2(\hat{s}-1)^2} + \mathcal{O}(\epsilon),
\end{aligned} \quad (2)$$

by introducing three dimensionless kinematic variables:

$$\hat{s} = \frac{(p_1+p_2)^2}{4m_b^2}, \quad \hat{t} = \frac{(p_1-p_3)^2}{4m_b^2}, \quad \hat{u} = \frac{(p_1-p_4)^2}{4m_b^2}, \quad (3)$$

and the reasonable approximation $M_{\Upsilon} = 2m_b$ is taken. Our LO results are consistent with those in Ref. [30]. The LO total cross section is obtained by convoluting the partonic cross section with the parton distribution function (PDF) in the proton:

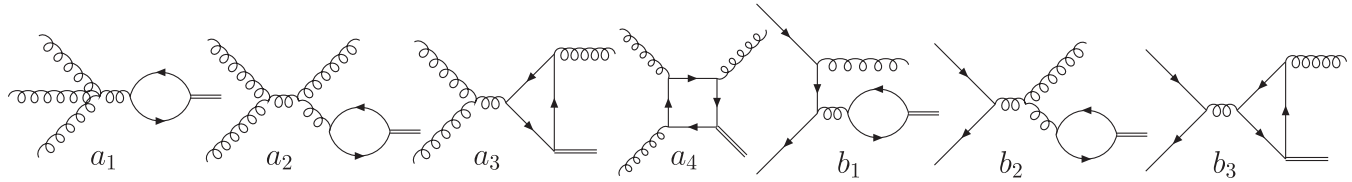

FIG. 1. Typical Feynman diagrams for LO processes. *a*) Feynman diagrams for process (L1); *b*) Feynman diagrams for processes (L2) and (L3). Diagrams in groups (a_1), (a_2), (b_1) and (b_2) are absent for the ${}^1S_0^{(8)}$ state.

$$\sigma^B[pp \to \Upsilon^{(8)} + X] = \sum_{i,j,k} \int \hat{\sigma}^B[i + j \to \Upsilon^{(8)} + k] \times G_{i/p}(x_1, \mu_f) G_{j/p}(x_2, \mu_f) dx_1 dx_2, \tag{4}$$

where $\Upsilon^{(8)}$ denotes a certain color-octet $\Upsilon[{}^1S_0^{(8)}]$ or $\Upsilon[{}^3S_1^{(8)}]$, μ_f is the factorization scale.

III. THE NLO CROSS SECTION

The NLO contributions can be written as a sum of two parts: one is the virtual corrections which arise from loop diagrams, the other is the real corrections caused by radiation of a real gluon, or a gluon splitting into a light quark-antiquark pair, or a light (anti)quark splitting into a light (anti) quark and a gluon.

A. Virtual corrections

There exist ultraviolet (UV), infrared (IR) and Coulomb singularities in the calculation of the virtual corrections. UV divergences from self-energy and triangle diagrams are canceled by introducing renormalization. Here we adopt the renormalization scheme used in Ref. [31]. The renormalization constants Z_m, Z_2, Z_{2l} and Z_3 which correspond to bottom quark mass m_b, bottom-field ψ_b, light quark field ψ_q and gluon field A_μ^a are defined in the on-mass-shell (OS) scheme while Z_g for the QCD gauge coupling constant α_s is defined in the modified-minimal-subtraction ($\overline{\text{MS}}$) scheme:

$$\begin{aligned}
\delta Z_m^{\text{OS}} &= -3C_F \frac{\alpha_s}{4\pi}\left[\frac{1}{\epsilon_{\text{UV}}} - \gamma_E + \ln\frac{4\pi\mu_r^2}{m_b^2} + \frac{4}{3}\right], \\
\delta Z_2^{\text{OS}} &= -C_F \frac{\alpha_s}{4\pi}\left[\frac{1}{\epsilon_{\text{UV}}} + \frac{2}{\epsilon_{\text{IR}}} - 3\gamma_E + 3\ln\frac{4\pi\mu_r^2}{m_b^2} + 4\right], \\
\delta Z_{2l}^{\text{OS}} &= -C_F \frac{\alpha_s}{4\pi}\left[\frac{1}{\epsilon_{\text{UV}}} - \frac{1}{\epsilon_{\text{IR}}}\right], \\
\delta Z_3^{\text{OS}} &= \frac{\alpha_s}{4\pi}\left[(\beta_0 - 2C_A)\left(\frac{1}{\epsilon_{\text{UV}}} - \frac{1}{\epsilon_{\text{IR}}}\right)\right], \\
\delta Z_g^{\overline{\text{MS}}} &= -\frac{\beta_0}{2}\frac{\alpha_s}{4\pi}\left[\frac{1}{\epsilon_{\text{UV}}} - \gamma_E + \ln(4\pi)\right],
\end{aligned} \tag{5}$$

where γ_E is the Euler's constant, $\beta_0 = \frac{11}{3}C_A - \frac{4}{3}T_F n_f$ is the one-loop coefficient of the QCD beta function and n_f is the number of active quark flavors. We have four light quarks u, d, s and c in our calculation, so $n_f = 4$. The color factors are given by $T_F = 1/2$, $C_F = 4/3$, $C_A = 3$ and μ_r is the renormalization scale.

There are 267 (for the ${}^1S_0^{(8)}$ state) and 413 (for the ${}^3S_1^{(8)}$ state) NLO diagrams for process (L1), including counter-term diagrams, while for both processes (L2) and (L3), there are 49 (for the ${}^1S_0^{(8)}$ state) and 111 (for the ${}^3S_1^{(8)}$ state) NLO diagrams. Part of the Feynman diagrams for these processes are shown in Fig. 2. The diagrams in which a virtual gluon line connects the quark pair contain Coulomb singularities, which can be isolated and attributed into renormalization of the $b\bar{b}$ wave function.

For each process, by summing over contributions from all diagrams, the virtual correction to the differential cross section can be expressed as

$$\frac{d\hat{\sigma}^V_{[L_i]}}{dt} \propto 2\,\text{Re}(M^B_{[L_i]} M^{V^*}_{[L_i]}), \tag{6}$$

where $M^B_{[L_i]}$ is the amplitude of process (L_i) at LO, and $M^V_{[L_i]}$ is the renormalized amplitude of corresponding process at NLO. $M^V_{[L_i]}$ is UV and Coulomb finite, but it still contains IR divergences. And the total cross section of virtual contribution could be written as

$$\sigma^V[pp \to \Upsilon^{(8)} + X] = \sum_{i,j,k} \int \hat{\sigma}^V[i + j \to \Upsilon^{(8)} + k] \times G_{i/p}(x_1, \mu_f) G_{j/p}(x_2, \mu_f) dx_1 dx_2. \tag{7}$$

B. Real corrections

There are eight processes involved in the real corrections:

$$gg \to \Upsilon[{}^1S_0^{(8)}, {}^3S_1^{(8)}]gg, \tag{R1}$$

$$gq \to \Upsilon[{}^1S_0^{(8)}, {}^3S_1^{(8)}]gq, \tag{R2}$$

$$q\bar{q} \to \Upsilon[{}^1S_0^{(8)}, {}^3S_1^{(8)}]gg, \tag{R3}$$

$$gg \to \Upsilon[{}^1S_0^{(8)}, {}^3S_1^{(8)}]q\bar{q}, \tag{R4}$$

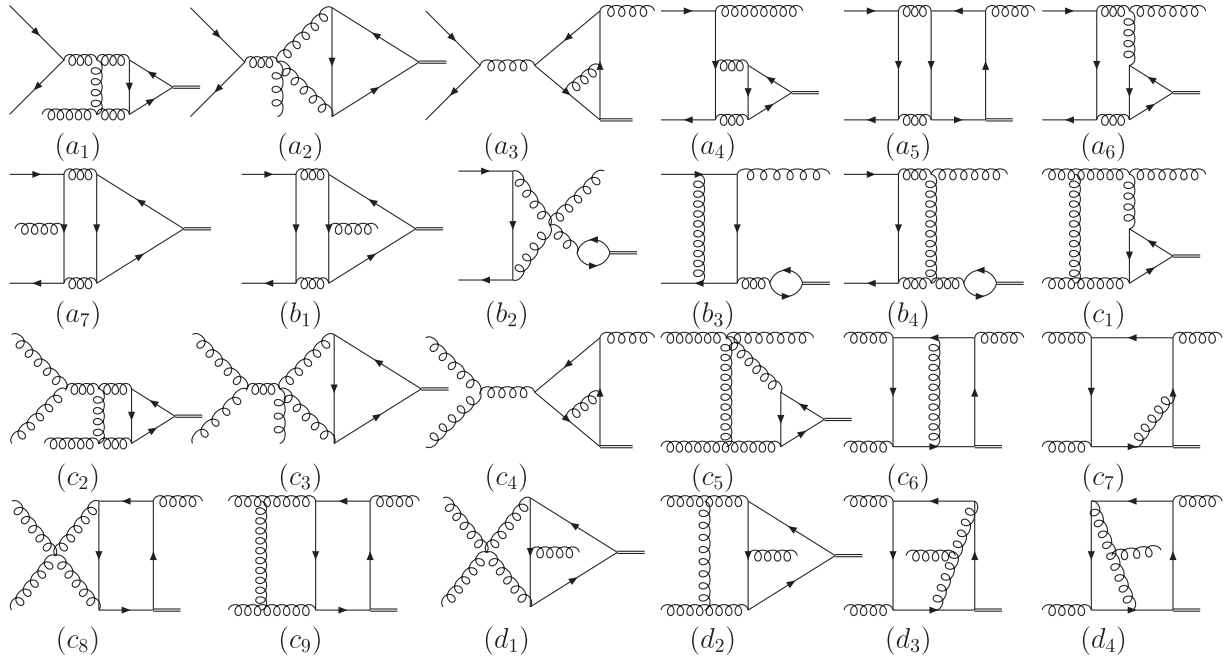

FIG. 2. Typical one-loop diagrams. *a*) Feynman diagrams for $gq \to \Upsilon[^1S_0^{(8)}]q$ and $q\bar{q} \to \Upsilon[^1S_0^{(8)}]g$; $a + b$) Feynman diagrams for $gq \to \Upsilon[^3S_1^{(8)}]q$ and $q\bar{q} \to \Upsilon[^3S_1^{(8)}]g$; *c*) Feynman diagrams for $gg \to \Upsilon[^1S_0^{(8)}]g$; $c + d$) Feynman diagrams for $gg \to \Upsilon[^3S_1^{(8)}]g$. Counter-term diagrams, together with corresponding loop diagrams, are not shown here.

$$q\bar{q} \to \Upsilon[^1S_0^{(8)}, {}^3S_1^{(8)}]q\bar{q}, \tag{R5}$$

$$q\bar{q} \to \Upsilon[^1S_0^{(8)}, {}^3S_1^{(8)}]q'\bar{q}', \tag{R6}$$

$$qq \to \Upsilon[^1S_0^{(8)}, {}^3S_1^{(8)}]qq, \tag{R7}$$

$$qq' \to \Upsilon[^1S_0^{(8)}, {}^3S_1^{(8)}]qq', \tag{R8}$$

where q, q' denote light quarks (antiquarks) with different flavors. Feynman diagrams for these processes are shown in Fig. 3.

We have neglected the contributions from two other processes, $gg \to \Upsilon^{(8)}b\bar{b}$ and $q\bar{q} \to \Upsilon^{(8)}b\bar{b}$, which are IR finite and small. Phase space integrations of the above eight processes generate IR singularities, which are either soft or collinear and can be conveniently isolated by slicing the phase space into different regions. We use the two-cutoff

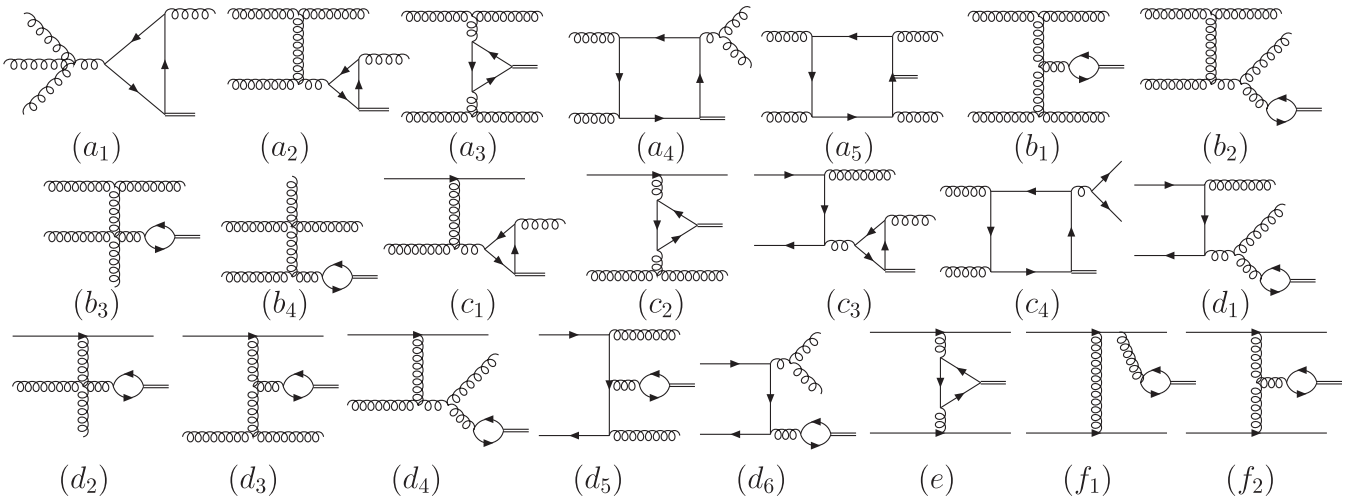

FIG. 3. Feynman diagrams for real correction processes. *a*) (R1) ($\Upsilon[^1S_0^{(8)}]$); $a + b$) (R1) ($\Upsilon[^3S_1^{(8)}]$); *c*) (R2) ~ (R4) ($\Upsilon[^1S_0^{(8)}]$); $c + d$) (R2) ~ (R4) ($\Upsilon[^3S_1^{(8)}]$); *e*) (R5) ~ (R8) ($\Upsilon[^1S_0^{(8)}]$); $e + f$) (R5) ~ (R8) ($\Upsilon[^3S_1^{(8)}]$). (R1) ($\Upsilon[^1S_0^{(8)}]$) denotes process $gg \to \Upsilon[^1S_0^{(8)}]gg$, (R1) ($\Upsilon[^3S_1^{(8)}]$) denotes process $gg \to \Upsilon[^3S_1^{(8)}]gg$, and so on.

phase space slicing method [32], which introduces two small cutoffs to decompose the phase space into three parts. Then the real cross section can be written as

$$\sigma^R = \sigma^S + \sigma^{\mathrm{HC}} + \sigma^{\mathrm{H\bar{C}}}. \tag{8}$$

It is easy to see that different parts of IR singularities from one real process can be factorized and each part should be added into the cross sections of different LO processes. This is the reason why we have to calculate the NLO corrections to the three LO processes together.

1. Soft

Soft singularities arise from real gluon emission. Thus only real processes (R1)–(R3) contain soft singularities, corresponding to the three LO processes. One should notice that, unlike the color-singlet case, the soft singularities caused by emitting a soft gluon from the quark pair in the S-wave color-octet states exist. We find that the factorized matrix element is the same as that in the case of emitting a soft gluon from a gluon.

Suppose p_5 is the momentum of the emitted gluon. If we define the Mandelstam invariants as $s_{ij} = (p_i + p_j)^2$ and $t_{ij} = (p_i - p_j)^2$, the soft region is defined in terms of the energy of p_5 in the $p_1 + p_2$ rest frame by $0 \le E_5 \le \delta_s\sqrt{s_{12}}/2$. For each of the three real processes, $\hat{\sigma}^S$ from the soft regions is calculated analytically under the soft approximation.

Following the similar factorization procedure as applied in the calculation of the color-singlet case [25], the matrix elements for a certain real process (R_i) in the soft region can be written as

$$|M_{[R_i]}|^2|_{\mathrm{soft}} \simeq -4\pi\alpha_s\mu_r^{2\epsilon}\sum_{j,k=1}^{4}\frac{-p_j\cdot p_k}{(p_j\cdot p_5)(p_k\cdot p_5)}M^{jk}_{[L_i]}, \tag{9}$$

with

$$M^{jk}_{[L_i]} = [\mathbf{T}^a(j)\mathbf{M}^{b_1\cdots b_{j'}\cdots b_4}_{[L_i]}]^\dagger[\mathbf{T}^a(k)\mathbf{M}^{b_1\cdots b_{k'}\cdots b_4}_{[L_i]}], \tag{10}$$

where $\mathbf{M}^{b_1\cdots b_4}_{[L_i]}$ is the color connected Born matrix element for LO processes (L_i). If the emitting parton j is an initial state quark or a final state antiquark, $\mathbf{T}^a(j) = T^a_{b_{j'}b_j}$. For an initial state antiquark or a final state quark $\mathbf{T}^a(j) = -T^a_{b_jb_{j'}}$. If the emitting parton j is a gluon or the color-octet state, $\mathbf{T}^a(j) = if_{ab_jb_{j'}}$. And the corresponding parton level differential cross section can be expressed as

$$d\hat{\sigma}^S_{[R_i]} = \left[\frac{\alpha_s}{2\pi}\frac{\Gamma(1-\epsilon)}{\Gamma(1-2\epsilon)}\left(\frac{4\pi\mu_r^2}{s_{12}}\right)^\epsilon\right]\sum_{j,k=1}^{4}d\hat{\sigma}^{jk}_{[L_i]}I^{jk}, \tag{11}$$

with

$$d\hat{\sigma}^{jk}_{[L_i]} = \frac{1}{2\Phi}\bar{\sum}M^{jk}_{[L_i]}d\Gamma_2. \tag{12}$$

The factor I^{jk} is universal for all three real processes, and is given in Appendix. A. Sometimes $d\hat{\sigma}^{jk}_{[L_i]}$ may be written in a more compact form as

$$d\hat{\sigma}^{jk}_{[L_i]} = C^{jk}_{[L_i]}d\hat{\sigma}^B_{[L_i]}, \tag{13}$$

where $C^{jk}_{[L_i]}$ is a constant. This is always true if the LO process (L_i) contains only one independent color factor in the matrix element. But for processes with two or more than two independent color factors, there seems to be no sure reason for it to be or not to be true. Of course, no matter whether Eq. (13) is true or not, we can always obtain $d\hat{\sigma}^{jk}_{[L_i]}$ through Eq. (12). Most processes involved in this calculation have more than one independent color factor, and they are listed in Appendix. (B 1).

2. Hard collinear

The hard collinear (HC) regions of the phase space are those where any invariant (s_{ij} or t_{ij}) becomes smaller in magnitude than $\delta_c s_{12}$. It is treated according to whether the singularities are from initial or final state emitting or splitting in the origin.

a. final state collinear For real processes (R1) ∼ (R6), which contain final state collinear singularities, the final state collinear region is defined by $0 \le s_{45} \le \delta_c s_{12}$. Again following the similar factorization procedure described in Ref. [32], the parton level cross section in the hard final state collinear region can be expressed as

$$\hat{\sigma}^{\mathrm{HC}}_f[R_i] = \hat{\sigma}^B[\mathrm{L}'_i]\left[\frac{\alpha_s}{2\pi}\frac{\Gamma(1-\epsilon)}{\Gamma(1-2\epsilon)}\left(\frac{4\pi\mu_r^2}{s_{12}}\right)^\epsilon\right]A_i^{\mathrm{HC}}. \tag{14}$$

For a certain real process (R_i), (L'_i) is the corresponding LO process it factorizes into. And the coefficient A_i^{HC} are listed in Table. I, with

TABLE I. The hard final state collinear factors for real correction processes and the corresponding LO processes.

R_i	L'_i	A_i^{HC}
$gg \to \Upsilon^{(8)}gg$	$gg \to \Upsilon^{(8)}g$	$\frac{1}{\epsilon}A_1^{g\to gg} + A_0^{g\to gg}$
$gq \to \Upsilon^{(8)}gq$	$gq \to \Upsilon^{(8)}q$	$\frac{1}{\epsilon}A_1^{q\to qg} + A_0^{q\to qg}$
$gg \to \Upsilon^{(8)}q\bar{q}$	$gg \to \Upsilon^{(8)}g$	$\frac{1}{\epsilon}A_1^{g\to q\bar{q}} + A_0^{g\to q\bar{q}}$
$q\bar{q} \to \Upsilon^{(8)}gg$	$q\bar{q} \to \Upsilon^{(8)}g$	$\frac{1}{\epsilon}A_1^{g\to gg} + A_0^{g\to gg}$
$q\bar{q} \to \Upsilon^{(8)}q\bar{q}$	$q\bar{q} \to \Upsilon^{(8)}g$	$\frac{1}{n_f}(\frac{1}{\epsilon}A_1^{g\to q\bar{q}} + A_0^{g\to q\bar{q}})$
$q\bar{q} \to \Upsilon^{(8)}q'\bar{q}'$	$q\bar{q} \to \Upsilon^{(8)}g$	$(1-\frac{1}{n_f})(\frac{1}{\epsilon}A_1^{g\to q\bar{q}} + A_0^{g\to q\bar{q}})$

$$
\begin{aligned}
A_1^{g\to gg} &= N(11/6+2\ln\delta_s'),\\
A_0^{g\to gg} &= N[67/18-\pi^2/3-\ln^2\delta_s'-\ln\delta_c(11/6+2\ln\delta_s')],\\
A_1^{q\to qg} &= C_F(3/2+2\ln\delta_s'),\\
A_0^{q\to qg} &= C_F[7/2-\pi^2/3-\ln^2\delta_s'-\ln\delta_c(3/2+2\ln\delta_s')],\\
A_1^{g\to q\bar{q}} &= -n_f/3,\\
A_0^{g\to q\bar{q}} &= n_f/3(\ln\delta_c-5/3),
\end{aligned}
\tag{15}
$$

and

$$
\delta_s' = \frac{s_{12}}{s_{12}+s_{45}-M_\Upsilon^2} \simeq \frac{\hat{s}}{\hat{s}-1}\delta_s. \tag{16}
$$

Thus the total cross section for real correction processes in hard final state collinear regions can be written as:

$$
\begin{aligned}
\sigma_f^{\rm HC} &= \sum_{i,j,k_1,k_2}\int \hat{\sigma}_f^{\rm HC}[i+j\to\Upsilon^{(8)}+k_1+k_2]\\
&\quad\times G_{i/p}(x_1,\mu_f)G_{j/p}(x_2,\mu_f)dx_1dx_2\\
&= \sum_{i,j,k}\int \hat{\sigma}^B[i+j\to\Upsilon^{(8)}+k]B^{\rm HC}(k)\\
&\quad\times G_{i/p}(x_1,\mu_f)G_{j/p}(x_2,\mu_f)dx_1dx_2,
\end{aligned}
\tag{17}
$$

where

$$
\begin{aligned}
B^{\rm HC}(g) &= \left[\frac{\alpha_s}{2\pi}\frac{\Gamma(1-\epsilon)}{\Gamma(1-2\epsilon)}\left(\frac{4\pi\mu_r^2}{s_{12}}\right)^\epsilon\right]\\
&\quad\times\left(\frac{A_1^{g\to gg}+A_1^{g\to q\bar{q}}}{\epsilon}+A_0^{g\to gg}+A_0^{g\to q\bar{q}}\right),\\
B^{\rm HC}(q) &= \left[\frac{\alpha_s}{2\pi}\frac{\Gamma(1-\epsilon)}{\Gamma(1-2\epsilon)}\left(\frac{4\pi\mu_r^2}{s_{12}}\right)^\epsilon\right]\left(\frac{A_1^{q\to qg}}{\epsilon}+A_0^{q\to qg}\right).
\end{aligned}
\tag{18}
$$

b. initial state collinear Almost all real processes, except process (R6), contain hard initial state collinear singularities. These singularities are partly absorbed into the redefinition of the PDF of the concerned hadrons (usually it is called the mass factorization [33]). Here we adopt the scale dependent PDF using the $\overline{\rm MS}$ convention given in Ref. [32].

$$
\begin{aligned}
G_{b/p}(x,\mu_f) &= G_{b/p}(x)-\frac{1}{\epsilon}\left[\frac{\alpha_s}{2\pi}\frac{\Gamma(1-\epsilon)}{\Gamma(1-2\epsilon)}\left(\frac{4\pi\mu_r^2}{\mu_f^2}\right)^\epsilon\right]\\
&\quad\times\int_x^1\frac{dz}{z}P_{bb'}(z)G_{b'/p}(x/z).
\end{aligned}
\tag{19}
$$

The second term is sometimes referred as the mass factorization counter-term. There is still something remaining after the cancellation, which can be expressed in two terms. The first one, which only exists in the real processes with a final state gluon, can be expressed as

$$
\hat{\sigma}_i^{\rm HC}[R_i] = \hat{\sigma}^B[L_i]\left[\frac{\alpha_s}{2\pi}\frac{\Gamma(1-\epsilon)}{\Gamma(1-2\epsilon)}\left(\frac{4\pi\mu_r^2}{\mu_f}\right)^\epsilon\right]A_i^{\rm SC},
$$

with

$$
\begin{aligned}
A_1^{\rm SC} &= 2A^{\rm SC}(g\to gg),\\
A_2^{\rm SC} &= A^{\rm SC}(q\to qg)+A^{\rm SC}(g\to gg),\\
A_3^{\rm SC} &= 2A^{\rm SC}(q\to qg),
\end{aligned}
\tag{20}
$$

and

$$
\begin{aligned}
A^{\rm SC}(q\to qg) &= \frac{1}{\epsilon}C_F[3/2+2\ln(\delta_s)],\\
A^{\rm SC}(g\to gg) &= \frac{1}{\epsilon}[2N\ln\delta_s+(11N-2n_f)/6],
\end{aligned}
\tag{21}
$$

where SC means it is from the soft collinear part in phase space. The corresponding hadronic total cross section is

$$
\begin{aligned}
\sigma_i^{\rm HC} &= \sum_{i,j,k}\int\hat{\sigma}_i^{\rm HC}[i+j\to\Upsilon^{(8)}+k+g]\\
&\quad\times G_{i/p}(x_1,\mu_f)G_{j/p}(x_2,\mu_f)dx_1dx_2\\
&= \sum_{i,j,k}\int\hat{\sigma}^B[i+j\to\Upsilon^{(8)}+k][B^{\rm SC}(i)+B^{\rm SC}(j)]\\
&\quad\times G_{i/p}(x_1,\mu_f)G_{j/p}(x_2,\mu_f)dx_1dx_2,
\end{aligned}
\tag{22}
$$

with

$$
\begin{aligned}
B^{\rm SC}(g) &= \left[\frac{\alpha_s}{2\pi}\frac{\Gamma(1-\epsilon)}{\Gamma(1-2\epsilon)}\left(\frac{4\pi\mu_r^2}{\mu_f}\right)^\epsilon\right]A^{\rm SC}(g\to gg),\\
B^{\rm SC}(q) &= \left[\frac{\alpha_s}{2\pi}\frac{\Gamma(1-\epsilon)}{\Gamma(1-2\epsilon)}\left(\frac{4\pi\mu_r^2}{\mu_f}\right)^\epsilon\right]A^{\rm SC}(q\to qg).
\end{aligned}
$$

The other term is obtained by summing up the remaining contributions from all the real correction processes. It can be written as

$$
\begin{aligned}
&\sigma_{add}^{\rm HC}[pp\to\Upsilon^{(8)}+X]\\
&\equiv\sum_{i,j,k}\int\hat{\sigma}^B[ij\to\Upsilon^{(8)}+k]\left[\frac{\alpha_s}{2\pi}\frac{\Gamma(1-\epsilon)}{\Gamma(1-2\epsilon)}\left(\frac{4\pi\mu_r^2}{s_{12}}\right)^\epsilon\right]\\
&\quad\times[G_{i/p}(x_1,\mu_f)\tilde{G}_{j/p}(x_2,\mu_f)+(x_1\leftrightarrow x_2)]dx_1dx_2,
\end{aligned}
\tag{23}
$$

with

$$
\tilde{G}_{c/p}(x,\mu_f) = \sum_{c'}\int_x^{1-\delta_s\delta_{cc'}}\frac{dy}{y}G_{c'/p}(x/y,\mu_f)\tilde{P}_{cc'}(y), \tag{24}
$$

and

$$
\tilde{P}_{ij}(y) = P_{ij}(y)\ln\left(\delta_c\frac{1-y}{y}\frac{s_{12}}{\mu_f^2}\right)-P_{ij}'(y). \tag{25}
$$

The n-dimensional unregulated ($y<1$) splitting functions $P_{ij}(y,\epsilon)$ has been written as $P_{ij}(y,\epsilon)=P_{ij}(y)+\epsilon P_{ij}'(y)$ with

$$
\begin{aligned}
P_{qq}(y) &= C_F \frac{1+y^2}{1-y}, \\
P'_{qq}(y) &= -C_F(1-y), \\
P_{gq}(y) &= C_F \frac{1+(1-y)^2}{y}, \\
P'_{qq}(y) &= -C_F y, \\
P_{gg}(y) &= 2N\left[\frac{y}{1-y} + \frac{1-y}{y} + y(1-y)\right], \\
P'_{gg}(y) &= 0, \\
P_{qg}(y) &= \frac{1}{2}[y^2 + (1-y)^2], \\
P'_{qg}(y) &= -y(1-y).
\end{aligned} \tag{26}
$$

C. Cross section of all NLO contributions

The hard noncollinear part $\sigma^{\mathrm{H\bar{C}}}$ is IR finite and can be numerically computed using the standard Monte-Carlo integration techniques. Now the real cross section can be expressed as

$$
\sigma^R = \sigma^S + \sigma_f^{\mathrm{HC}} + \sigma_i^{\mathrm{HC}} + \sigma_{add}^{\mathrm{HC}} + \sigma^{\mathrm{H\bar{C}}}. \tag{27}
$$

And we have

$$
\sigma^{\mathrm{NLO}} = \sigma^B + \sigma^V + \sigma^R. \tag{28}
$$

IV. TRANSVERSE MOMENTUM DISTRIBUTION

To obtain the transverse momentum p_t distribution of Υ, a similar transformation for integration variables ($dx_2 dt \to J dp_t dy$) which we introduced in our previous work [25] is applied. Therefore we have

$$
\frac{d\sigma}{dp_t} = \sum_{i,j} \int J dx_1 dy G_{i/p}(x_1, \mu_f) G_{j/p}(x_2, \mu_f) \frac{d\hat{\sigma}}{dt}, \tag{29}
$$

with

$$
\begin{aligned}
&p_1 = x_1 \frac{\sqrt{S}}{2}(1,0,0,1), \qquad p_2 = x_2 \frac{\sqrt{S}}{2}(1,0,0,-1), \\
&m_t = \sqrt{M_\Upsilon^2 + p_t^2}, \qquad p_3 = (m_t \cosh y, p_t, 0, m_t \sinh y), \\
&x_t = \frac{2m_t}{\sqrt{S}}, \qquad \tau = \frac{m_4^2 - M_\Upsilon^2}{\sqrt{S}}, \qquad J = \frac{4x_1 x_2 p_t}{2x_1 - x_t e^y}, \\
&x_2 = \frac{2\tau + x_1 x_t e^{-y}}{2x_1 - x_t e^y}, \qquad x_1|_{\min} = \frac{2\tau + x_t e^y}{2 - x_t e^{-y}},
\end{aligned} \tag{30}
$$

where $\sqrt{S}$ is the center-of-mass energy of $p\bar{p}(p)$ at the Tevatron or LHC, m_4 is the invariant mass of all the final state particles except Υ, and y and p_t are the rapidity and transverse momentum of Υ in the laboratory frame, respectively.

V. POLARIZATION

The polarization parameter α is defined as:

$$
\alpha(p_t) = \frac{d\sigma_T/dp_t - 2d\sigma_L/dp_t}{d\sigma_T/dp_t + 2d\sigma_L/dp_t}. \tag{31}
$$

It represents the measurement of Υ polarization as a function of Υ transverse momentum p_t when calculated at each point in p_t distribution. To evaluate $\alpha(p_t)$, the polarization of Υ must be explicitly retained in the calculation. The partonic differential cross section for a polarized Υ is expressed as:

$$
\frac{d\hat{\sigma}_\lambda}{dt} = a\epsilon(\lambda)\cdot\epsilon^*(\lambda) + \sum_{i,j=1,2} a_{ij} p_i \cdot \epsilon(\lambda) p_j \cdot \epsilon^*(\lambda), \tag{32}
$$

where $\lambda = T_1, T_2, L$. $\epsilon(T_1)$, $\epsilon(T_2)$, $\epsilon(L)$ are the two transverse and longitudinal polarization vectors of Υ respectively, and the polarizations of all the other particles are summed over in n dimensions. One can find that a and a_{ij} are finite when the virtual corrections and real corrections are properly handled as aforementioned. Therefore, there is no difference in the differential cross section $d\hat{\sigma}_\lambda/dt$ whether the polarization of Υ is summed over in 4 or n dimensions. Thus we can just treat the polarization vectors of Υ in 4 dimensions, and also the spin average factor goes back to 4 dimensions. The gauge invariance is explicitly checked by replacing the gluon polarization vector into its 4-momentum in the final numerical calculation.

VI. NUMERICAL RESULT

In our numerical computations, the CTEQ6L1 and CTEQ6M PDFs [34], and the corresponding fitted value $\alpha_s(M_Z) = 0.130$ and $\alpha_s(M_Z) = 0.118$ are used for LO and NLO calculations, respectively. The bottom quark mass is set as 4.75 GeV, and the branch ratio $\mathrm{Br}(\Upsilon \to \mu^+\mu^-) = 0.0248$ [35] is used.

The choice of the renormalization scale μ_r and factorization scale μ_f is an important issue in the calculations, and it causes uncertainties. We choose $\mu_r = \mu_f = \mu_0 \equiv \sqrt{(2m_b)^2 + p_t^2}$ as our default choice. And the center-of-mass energies are chosen as 1.8 and 1.96 TeV for Tevatron Run I and Run II, respectively. For the LHC, it is chosen as 14 TeV.

At first, different values of the two cutoffs, δ_s and δ_c, are used to check the independence of the final results on the cutoffs and the invariance is observed within the error tolerance. Then the two phase space cutoffs are fixed as $\delta_s = 10^{-3}$ and $\delta_c = \delta_s/50$ in the following calculations.

It is known that the QCD perturbative expansion is not good in the regions of small transverse momentum or large rapidity of Υ. Therefore, the results are restricted in the region $p_t > 3$. For the rapidity cut, $|y| < 3$ is chosen at the

LHC, while at the Tevatron $|y| > 0.4$, $|y| < 0.6$ or $|y| < 1.8$ is used according to various experimental data.

To fix the NRQCD matrix elements for color-octet states of $\Upsilon(1S)$, data from both CDF and D0 [36,37] is used, and the fitting starts from Eq. (4) of Ref. [38] where the contributions from spin-singlet states $\eta_b(nS)$ and $h_b(nS)$ are not included. And we have to take a few approximations in our fitting procedure:

(i) For the S-wave color-singlet part, only the direct color-singlet $\Upsilon(1S)$ and feed-down from $\Upsilon(2S)$ are considered, while other contributions have been neglected. The contribution from the feed-down of $\Upsilon(2S)$ can be included to the direct $\Upsilon(1S)$ production by multiplying a factor of $\mathrm{Br}[\Upsilon(2S) \to \Upsilon(1S) + X] \times \langle \mathcal{O}_1^{\Upsilon}(2S)\rangle / \langle \mathcal{O}_1^{\Upsilon}(1S)\rangle$, which results in a factor of 1.127 after a short calculation with PDG data [35]. And the results for direct $\Upsilon(1S)$ of color-singlet contribution are extracted from our previous work [25].

(ii) The contributions from P-wave color-singlet states $\chi_{bJ}(nP)$ are estimated by multiplying a decay fraction $F^{\Upsilon(1S)}_{\chi_b(nP)} \approx F^{\Upsilon(1S)}_{\chi_b(1P)} + F^{\Upsilon(1S)}_{\chi_b(2P)}$, where $F^{\Upsilon(1S)}_{\chi_b(1P)}$ and $F^{\Upsilon(1S)}_{\chi_b(2P)}$ can be obtained from an older sample with the cuts $p_t > 8$ and $|y_\Upsilon| < 0.4$ [39]. As pointed out in Ref. [29], the fraction does not depend very strongly on p_t according to Fig. 2 of Ref. [37]. Also, from Fig. 4 of Ref. [36] we can see it does not depend very strongly on the rapidity cut either. Thus $F^{\Upsilon(1S)}_{\chi_b(1P)} = 27.1 \pm 6.9 \pm 4.4\%$ and $F^{\Upsilon(1S)}_{\chi_b(2P)} = 10.5 \pm 4.4 \pm 1.4\%$ are taken in our calculation, which result in $F^{\Upsilon(1S)}_{\chi_b(nP)} \approx 37.6 \pm 9.4\%$.

(iii) The contribution from P-wave color-octet states $\Upsilon[^3P_J^{(8)}]$ at NLO are still not available. As shown below, the NLO QCD corrections to $\Upsilon[^1S_0^{(8)}]$ do not change the cross section very much. If we assume that the NLO QCD corrections to $\Upsilon[^3P_J^{(8)}]$ are also small, we can mix it with $\Upsilon[^1S_0^{(8)}]$ again, like what we have done at LO. Thus, the value of our fitted $\langle \mathcal{O}_8^{\Upsilon}(^1S_0)\rangle_{\mathrm{inc}}$ includes the contributions from $\Upsilon[^3P_J^{(8)}]$ as well.

With these approximations, the formula we used for the fitting of inclusive color-octet matrix elements becomes

$$\begin{aligned} d\sigma[\Upsilon]_{\mathrm{inc}} = {} & 1.127 \times d\sigma[(b\bar{b})_1(^3S_1)]\langle \mathcal{O}_1^{\Upsilon}(^3S_1)\rangle \\ & + F^{\Upsilon(1S)}_{\chi_b(nP)} d\sigma[\Upsilon]_{\mathrm{inc}} + d\sigma[(b\bar{b})_8(^1S_0)] \\ & \times \langle \mathcal{O}_8^{\Upsilon}(^1S_0)\rangle_{\mathrm{inc}} + d\sigma[(b\bar{b})_8(^3S_1)] \\ & \times \langle \mathcal{O}_8^{\Upsilon}(^3S_1)\rangle_{\mathrm{inc}}. \end{aligned} \tag{33}$$

By fitting the CDF and D0 data, the inclusive NRQCD matrix elements for color-octet states $\langle \mathcal{O}_8^{\Upsilon}\rangle_{\mathrm{inc}}$ is obtained, as shown in Table. II. Here and hereafter all the mentioned fittings are done by using the multiple linear regression method.

TABLE II. The fitting results for inclusive NRQCD matrix elements for color-octet states $\langle \mathcal{O}_8^{\Upsilon}\rangle_{\mathrm{inc}}$ (in unit of 10^{-2} GeV^3). Here ndf stands for number of degrees of freedom.

	CDF	D0
$\langle \mathcal{O}_8^{\Upsilon}(^1S_0)\rangle_{\mathrm{inc}}$	1.646 ± 0.661	1.220 ± 0.448
$\langle \mathcal{O}_8^{\Upsilon}(^3S_1)\rangle_{\mathrm{inc}}$	5.175 ± 0.845	4.375 ± 0.529
R^2	0.93614	0.97745
$\bar{R}^2$	0.92017	0.96617
χ^2/ndf	8.847/8	2.909/4

The uncertainty in $F^{\Upsilon(1S)}_{\chi_b(nP)}$ is considered. And the experimental error in the p_t distribution data is also considered, which is negligible comparing with the former one when fitting the D0 data. R^2 is the coefficient of determination of fitting and $\bar{R}^2$ is the adjusted coefficient of determination. The fitting results are shown in Figs. 4 and 5, together with our predictions for inclusive Υ production at the LHC. The bands in the figure also contain the uncertainty from the scale dependence. This part of the uncertainty is obtained through following procedure. We generate five groups of data, with $\mu_r = \mu_f = \mu_0, 2\mu_r = 2\mu_f = \mu_0, \mu_r = \mu_f = 2\mu_0, 4\mu_r = \mu_f = 2\mu_0$ and $\mu_r = 4\mu_f = 2\mu_0$, and the uncertainty covers the maximum and minimum range of the data. This kind of uncertainty has been included in all the bands of the following figures too.

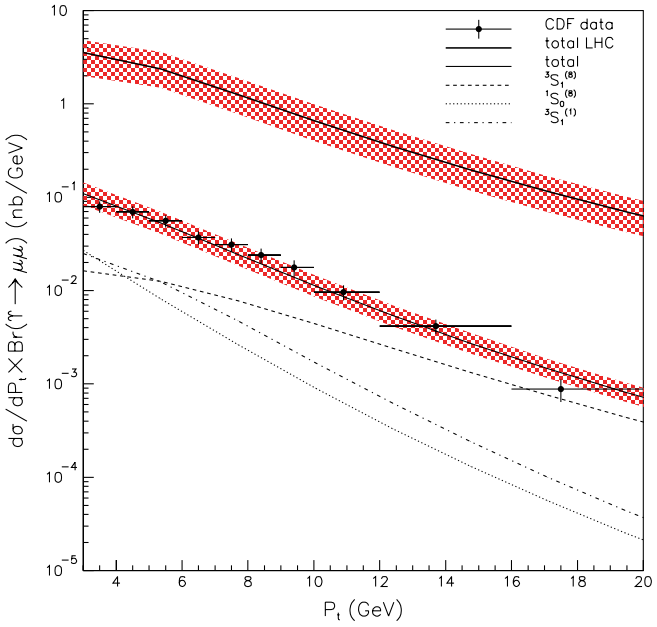

FIG. 4 (color online). The transverse momentum distribution of inclusive Υ production at the Tevatron and LHC. The CDF data is from Ref. [37]. The c.m.s energy and rapidity cut for Tevatron is $\sqrt{s} = 1.8$ TeV and $|y| < 0.4$.

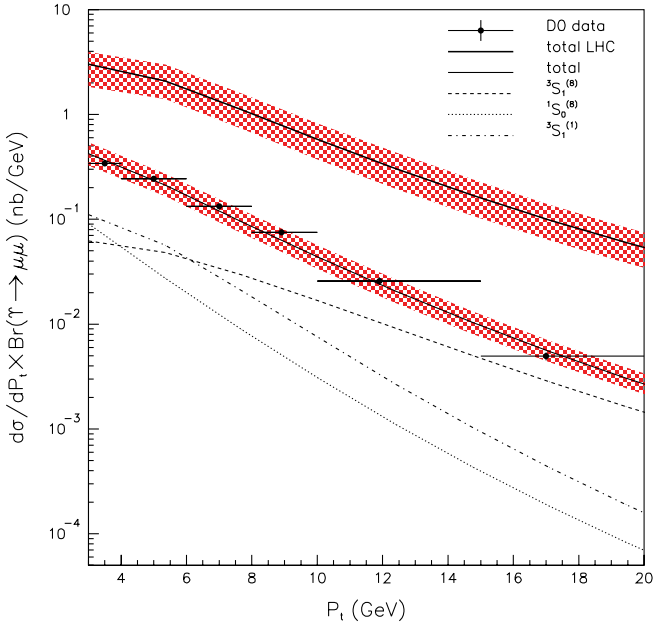

FIG. 5 (color online). The transverse momentum distribution of inclusive Υ production at the Tevatron and LHC. The D0 data is from Ref. [36]. The c.m.s energy and rapidity cut for Tevatron is $\sqrt{s} = 1.96$ TeV and $|y| < 1.8$.

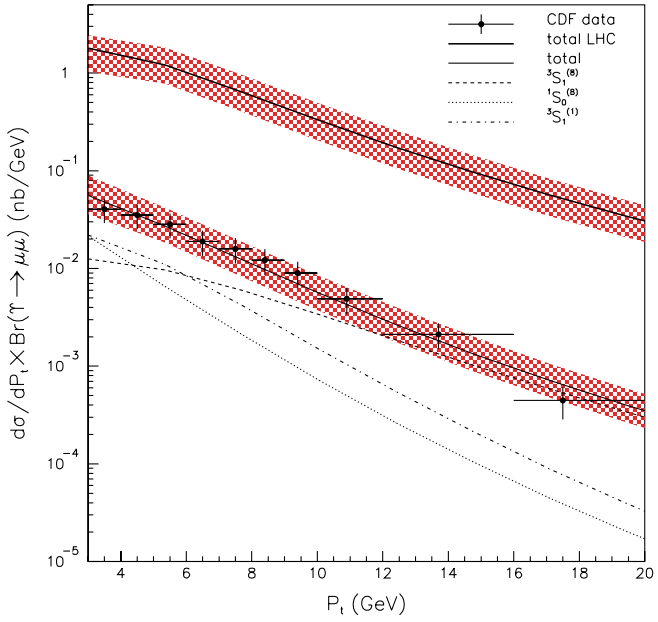

FIG. 6 (color online). The transverse momentum distribution of direct Υ production at the Tevatron and LHC. The CDF data is from Ref. [37]. The c.m.s energy and rapidity cut for Tevatron is $\sqrt{s} = 1.8$ TeV and $|y| < 0.4$.

The direct fraction of direct Υ production can also be obtained from Ref. [39] as $F_{\rm dir}^{\Upsilon(1S)} = 50.9 \pm 12.2\%$. Thus we can use the formula

$$F_{\rm dir}^{\Upsilon(1S)} d\sigma[\Upsilon]_{\rm inc} = d\sigma[(b\bar{b})_1(^3S_1)]\langle \mathcal{O}_1^{\Upsilon}(^3S_1)\rangle + d\sigma[(b\bar{b})_8(^1S_0)]\langle \mathcal{O}_8^{\Upsilon}(^1S_0)\rangle + d\sigma[(b\bar{b})_8(^3S_1)]\langle \mathcal{O}_8^{\Upsilon}(^3S_1)\rangle, \quad (34)$$

to fit the direct color-octet matrix elements. The fitted results for direct NRQCD matrix elements for color-octet states $\langle \mathcal{O}_8^{\Upsilon}\rangle$ is shown in Table. III.

The uncertainty comes from $F_{\rm dir}^{\Upsilon(1S)}$ and the measured p_t distribution data. Again the value of our fitted $\langle \mathcal{O}_8^{\Upsilon}(^1S_0)\rangle$ includes the contribution from $\Upsilon[^3P_J^{(8)}]$. The fitting results are shown in Figs. 6 and 7, together with our prediction for direct Υ production at the LHC.

TABLE III. The fitting results for direct NRQCD matrix elements for color-octet states $\langle \mathcal{O}_8^{\Upsilon}\rangle$ (in unit of 10^{-2} GeV^3).

	CDF	D0
$\langle \mathcal{O}_8^{\Upsilon}(^1S_0)\rangle$	1.316 ± 0.558	0.861 ± 0.352
$\langle \mathcal{O}_8^{\Upsilon}(^3S_1)\rangle$	3.982 ± 0.673	3.533 ± 0.415
R^2	0.928 96	0.977 56
$\bar{R}^2$	0.911 20	0.966 35
χ^2/ndf	4.860/8	1.062/4

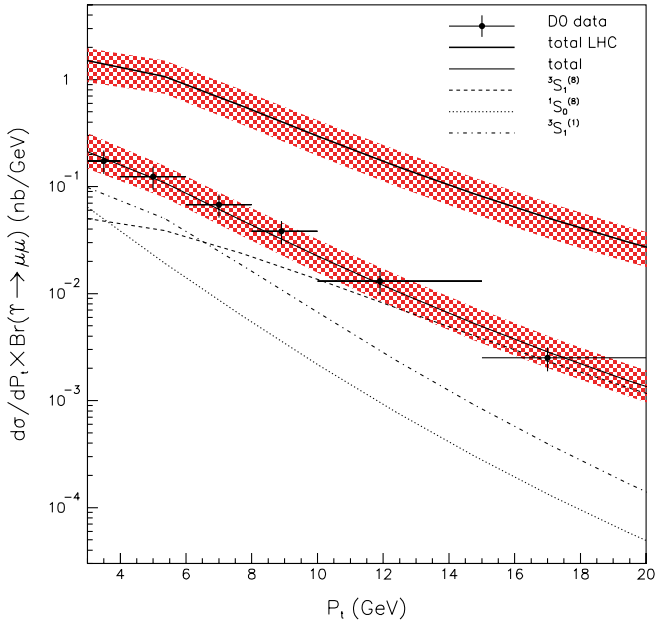

FIG. 7 (color online). The transverse momentum distribution of direct Υ production at the Tevatron and LHC. The D0 data is from Ref. [36]. The c.m.s energy and rapidity cut for Tevatron is $\sqrt{s} = 1.96$ TeV and $|y| < 1.8$.

From the data in Tables. II and III, we can see that the two fittings are consistent with each other while the fitting with the D0 data shows more goodness. The D0 data is obtained from larger data sample, and contained much

smaller uncertainty in the p_t distribution measurement. Thus, even though the CDF measurement has more data points, we choose the results obtained from the D0 data for our further predictions.

The dependence of the total cross section on the renormalization scale μ_r and factorization scale μ_f are shown in Fig. 8. It is obvious that the NLO QCD corrections make such dependence milder. We can also see that the NLO QCD corrections effect the cross section less at the LHC than at the Tevatron.

The p_t distributions of Υ production via S-wave color-octet states at LO and NLO are presented in Figs. 9 and 10 to show how much the corrections are. And we see that only slight changes appear when the NLO QCD corrections are included.

$\Upsilon[^1S_0^{(8)}]$ hadronize into unpolarized Υ, so it contributes to $\alpha = 0$ for both the LO and NLO. The p_t distributions of Υ polarization parameter α from $\Upsilon[^3S_1^{(8)}]$ are shown in Fig. 11, and there is a slight change when the NLO corrections are taken into account. Our predictions for the polarization of direct Υ production are also presented in the figure as a "total" result.

In Fig. 12, the polarization of inclusive Υ production at the Tevatron is shown. As the polarization of Υ from the feed-down of $\chi_b(nP)$ is not available yet, a huge band is obtained by verifying the polarization of this part between

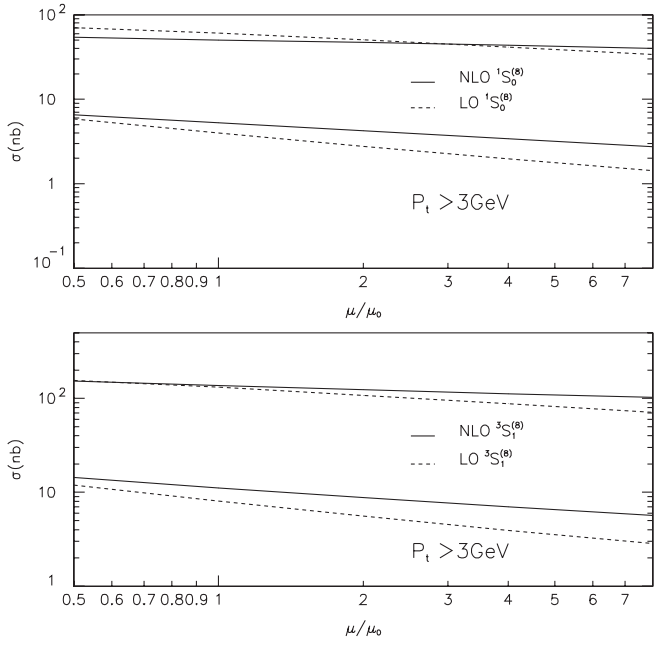

FIG. 8. The total cross section of Υ hadroproduction at the LHC (upper curves) and Tevatron (lower curves), as function of μ with $\mu_r = \mu_f = \mu$ and $\mu_0 = \sqrt{(2m_b)^2 + p_t^2}$. The c.m.s energy and rapidity cut for Tevatron is $\sqrt{s} = 1.96$ TeV and $|y| < 1.8$. And "total cross section" here means the differential cross section integrated in p_t from 3 GeV.

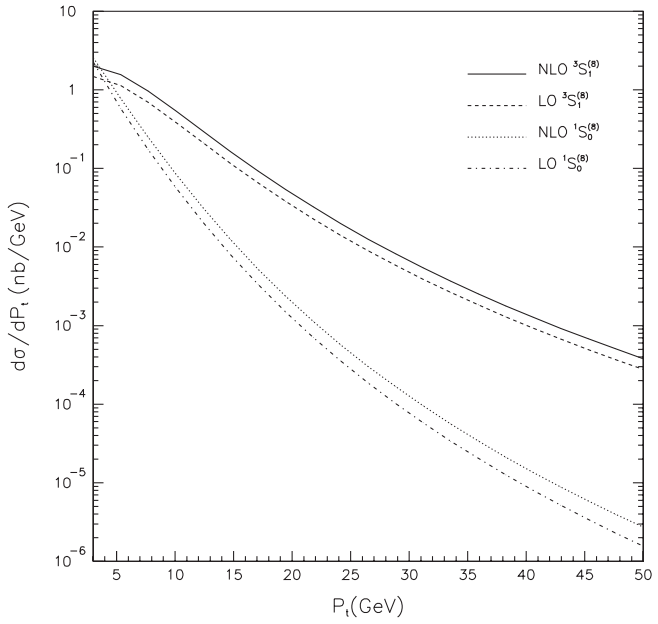

FIG. 9. The LO and NLO transverse momentum distribution of Υ production via CO transition with $\mu_r = \mu_f = \mu_0$ at the Tevatron.

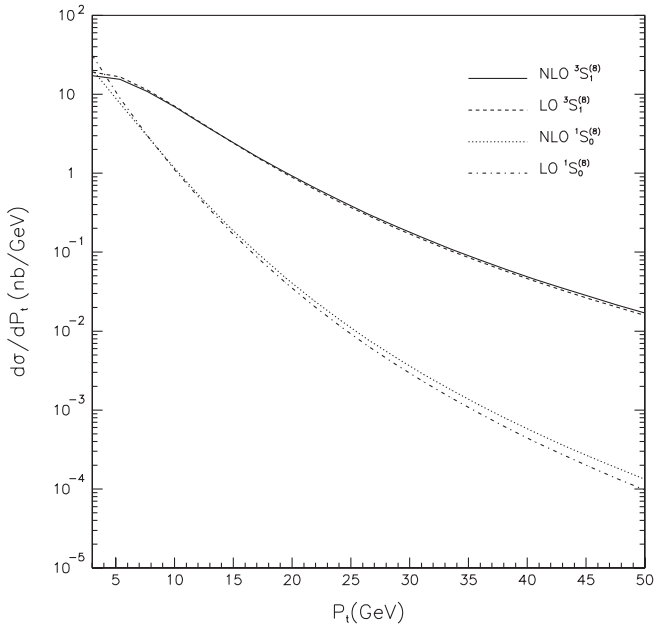

FIG. 10. The LO and NLO transverse momentum distribution of Υ production via CO transition with $\mu_r = \mu_f = \mu_0$ at the LHC.

-1 and 1. The experimental data from the D0 [21] and CDF [40] is also shown. We can see that, there is still some distance between the theoretical prediction and experimental measurement, even with such a large band. From the figure, as well as Fig. 11, it is obvious that the difference of

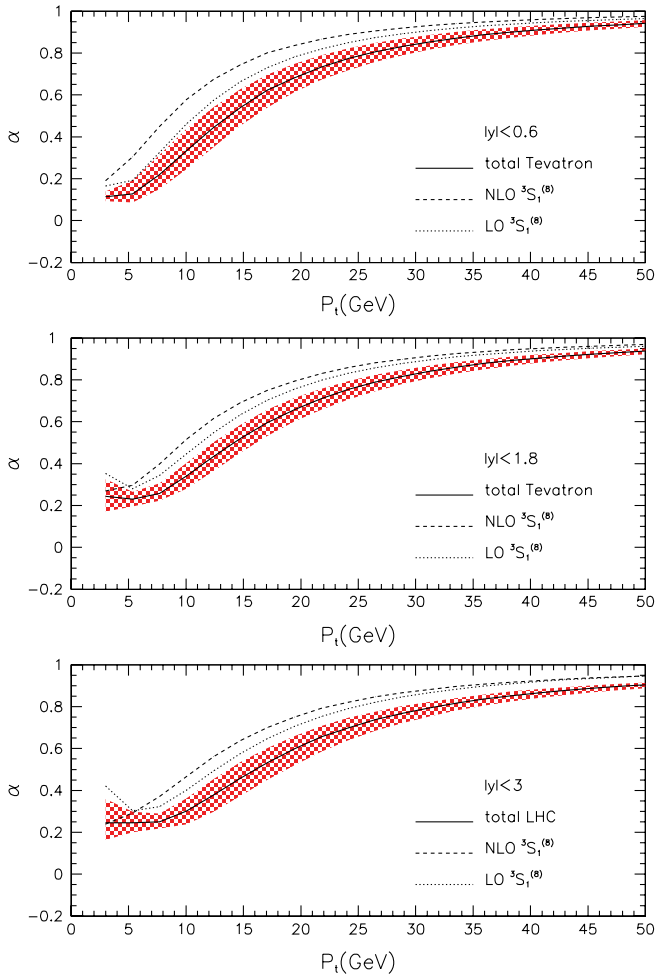

FIG. 11 (color online). The transverse momentum distribution of polarization parameter α for direct Υ production at the Tevatron and LHC. The c.m.s. energies and rapidity cuts (from the top down) are: 1) $\sqrt{s} = 1.96$ TeV and $|y| < 0.6$; 2) $\sqrt{s} = 1.96$ TeV and $|y| < 1.8$; 3) $\sqrt{s} = 14$ TeV and $|y| < 3$.

rapidity cut does not change the polarization status very much. Thus the discrepancy between the data of CDF and D0 may not be caused by this reason.

VII. Υ(3S)

In order to get rid of the large uncertainty rising from the unknown polarization status of Υ from the feed-down of $\chi_b(nP)$, we apply our calculation to the case of Υ(3S). We take $m_c = M_{\Upsilon(3S)}/2 = 5.18$ GeV as an approximation, and the branch ratio $\mathrm{Br}(\Upsilon(3S) \to \mu^+\mu^-) = 0.0218$ [35] is used. The wave function at the origin is chosen $|R_s^{\Upsilon(3S)}(0)|^2 = 2.474\ \mathrm{GeV}^3$. Thus the NRQCD color-octet matrix elements for $\langle \mathcal{O}_8^{\Upsilon(3S)} \rangle$ can be obtained by fitting the CDF data [37] with $\sqrt{s} = 1.8$ TeV and $|y| < 0.4$ using

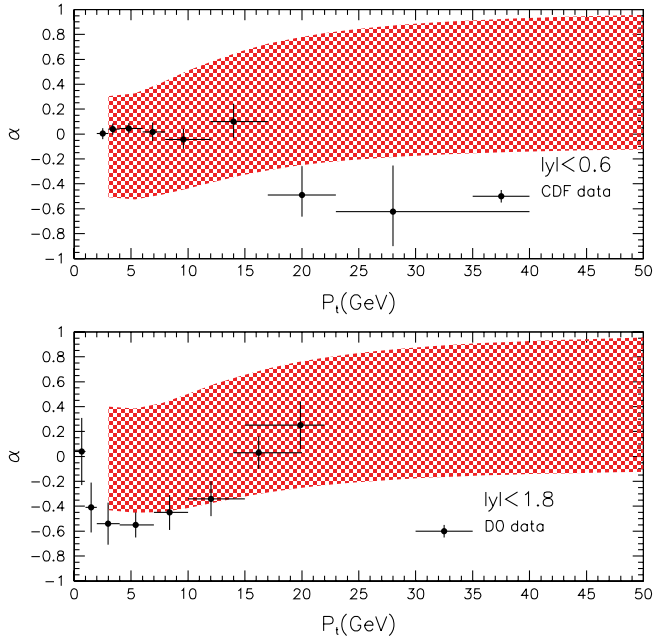

FIG. 12 (color online). The transverse momentum distribution of polarization parameter α for inclusive Υ production at the Tevatron. The c.m.s is chosen as 1.96 TeV, and the rapidity cuts in two figures are $|y| < 0.6$ (upper) and $|y| < 1.8$ (lower), respectively. The CDF data is from Ref. [40] while the D0 data is from Ref. [21].

$$d\sigma[\Upsilon(3S)] = d\sigma[(b\bar{b})_1(^3S_1)]\langle \mathcal{O}_1^{\Upsilon(3S)}(^3S_1)\rangle + d\sigma[(b\bar{b})_8(^1S_0)]\langle \mathcal{O}_8^{\Upsilon(3S)}(^1S_0)\rangle + d\sigma[(b\bar{b})_8(^3S_1)]\langle \mathcal{O}_8^{\Upsilon(3S)}(^3S_1)\rangle. \quad (35)$$

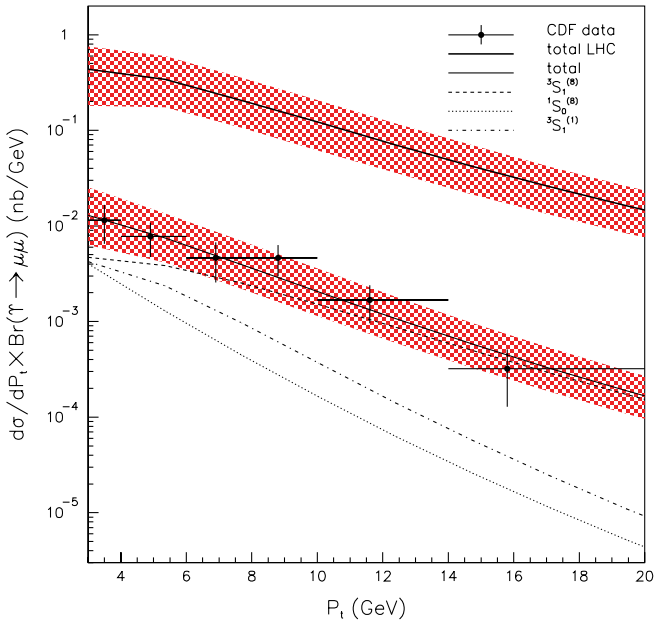

FIG. 13 (color online). The transverse momentum distribution of Υ(3S) production at the Tevatron and LHC. The CDF data is from Ref. [37].

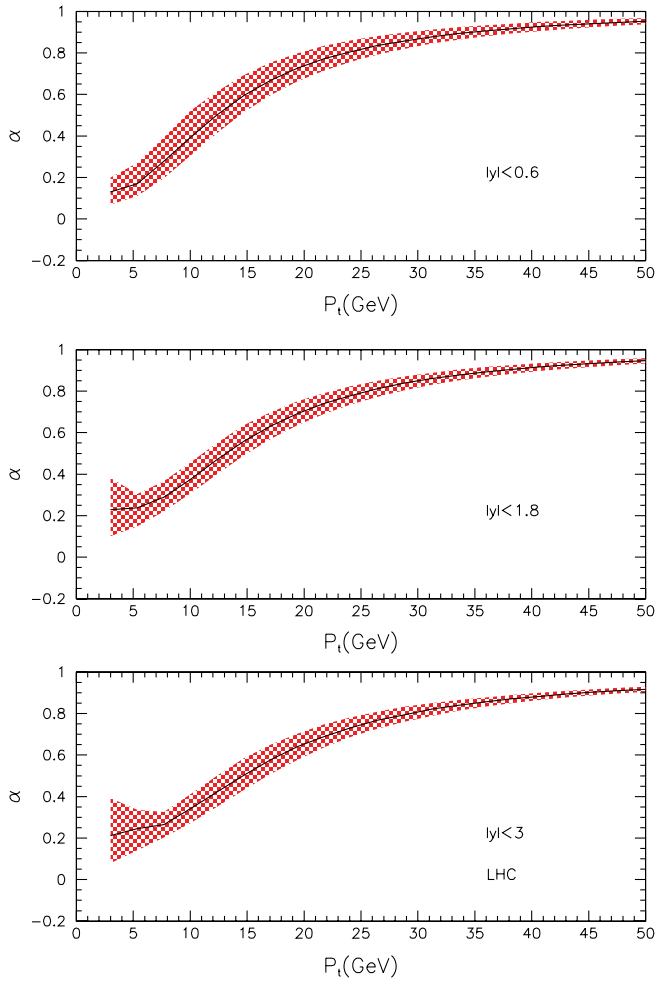

FIG. 14 (color online). The transverse momentum distribution of polarization parameter α for $\Upsilon(3S)$ production at the Tevatron and LHC. The c.m.s. energies and rapidity cuts (from the top down) are: 1) $\sqrt{s} = 1.96$ TeV and $|y| < 0.6$; 2) $\sqrt{s} = 1.96$ TeV and $|y| < 1.8$; 3) $\sqrt{s} = 14$ TeV and $|y| < 3$.

The fitted matrix elements are

$$\begin{aligned} \langle \mathcal{O}_8^{\Upsilon}(^1S_0)\rangle &= (0.460 \pm 0.484) \times 10^{-2}\ \text{GeV}^3 \\ \langle \mathcal{O}_8^{\Upsilon}(^3S_1)\rangle &= (3.250 \pm 0.876) \times 10^{-2}\ \text{GeV}^3, \end{aligned} \tag{36}$$

with $R^2 = 0.90665$ and $\bar{R}^2 = 0.85997$. Only the error in the experimental data is considered in the fitting. The fitting results are shown in Fig. 13, together with our prediction for $\Upsilon(3S)$ production at the LHC. The bands in the figure contain uncertainty from both the matrix elements and scale dependence.

Our predictions for the polarization of $\Upsilon(3S)$ production at the Tevatron and LHC are shown in Fig. 14. Even though the center-of-mass system (c.m.s.) energy and rapidity cut are different, the behavior of polarization parameter α is similar, especially in high P_t regions.

VIII. SUMMARY AND DISCUSSION

In summary, in this work, we have calculated the NLO QCD corrections to Υ production via S-wave color-octet states $\Upsilon[^1S_0^{(8)}, {}^3S_1^{(8)}]$ at the Tevatron and LHC. With $\mu_r = \mu_f = \mu_0$, the K factors of total cross section (ratio of NLO to LO) are 1.313 and 1.379 for $\Upsilon[^1S_0^{(8)}]$ and $\Upsilon[^3S_1^{(8)}]$ at the Tevatron, while at the LHC they are 1.044 and 1.182, respectively. Unlike for the color-singlet case, there are only slight changes to the transverse momentum distributions of Υ production and the Υ polarization when the NLO QCD corrections are taken into account. All the results imply that the perturbative QCD expansion quickly converges for Υ production via the S-wave color-octet states, in contrast with that via color-singlet, where the NLO contributions are too large to hint a good convergence at the next-to-next-to-leading order. By fitting the experimental data from the CDF and D0 Collaborations at the Tevatron, the matrix elements for S-wave color-octet states are obtained. And new predictions for the p_t distributions of the $\Upsilon(1S)$ production and polarization at the Tevatron and LHC are presented. The prediction for the polarization of inclusive $\Upsilon(1S)$ contains large uncertainty rising from the unknown polarization of $\Upsilon(1S)$ from feed-down of χ_b. Even with such a large uncertainty, there are still some distance between the prediction and experiment data. Also, the errors of the fractions used in the fitting, $F_{\chi_b(1P)}^{\Upsilon(1S)}$, $F_{\chi_b(2P)}^{\Upsilon(1S)}$ and $F_{\text{dir}}^{\Upsilon(1S)}$, are quite large and result in large uncertainty in the matrix elements. New measurements on the production and polarization for direct $\Upsilon(1S)$ are expected. The production of $\Upsilon(3S)$ at the Tevatron and LHC is also studied in order to get rid of the large uncertainty from the unknown χ_b feed-down, and there is large uncertainty in the fitted matrix elements because of the large uncertainty in current experimental data. Our prediction for the polarization of $\Upsilon(3S)$ production at the hadron colliders is also presented. Further measurements on the production of $\Upsilon(3S)$ and its polarization is also expected.

ACKNOWLEDGMENTS

This work is supported by the National Natural Science Foundation of China (Nos. 10475083, 10979056, 10935012 and 11005137), by the Chinese Academy of Science under Project No. INFO-115-B01, and by the China Postdoctoral Science Foundation Grant No. 20090460535.

APPENDIX A: CALCULATION OF THE FACTOR I^{jk}

If we write the n-momentum of soft gluon in the $p_1 + p_2$ rest frame as

$$p_5 = E_5(1, \ldots, \sin\theta_1 \cos\theta_2, \cos\theta_1), \tag{A1}$$

then I^{jk} is defined as

$$I^{jk} = \int \frac{-(p_j \cdot p_k)}{(p_j \cdot p_5)(p_k \cdot p_5)} dS, \tag{A2}$$

with

$$dS = \frac{1}{\pi}\left(\frac{4}{s_{12}}\right)^{-\epsilon} \times \int_0^{\delta_s\sqrt{s_{12}}/2} dE_5 E_5^{1-2\epsilon} \sin^{1-2\epsilon}\theta_1 d\theta_1 \sin^{-2\epsilon}\theta_2 d\theta_2. \tag{A3}$$

Before the calculation of I^{jk}, define β_j as $\beta_j = |\vec{p}_j|/E_j$, which is the ratio of momentum to energy of particle i in the $p_1 + p_2$ rest frame, where

$$\beta_1 = \beta_2 = \beta_4 = 1, \qquad \beta_3 = \frac{\hat{s}-1}{\hat{s}+1} \equiv \beta. \tag{A4}$$

Then we can write p_j and p_k as

$$\begin{aligned} p_j &= E_j(1, \cdots, \beta_j) \\ p_k &= E_k(1, \cdots, \beta_k \sin\theta_{jk}, \beta_k \cos\theta_{jk}), \end{aligned} \tag{A5}$$

where θ_{jk} is the angle between j and k. Now we have

$$I^{jk} = -\frac{1-\beta_j\beta_k\cos\theta}{\pi} I_E I_A^{jk}, \tag{A6}$$

where

$$I_E = \left(\frac{4}{s_{12}}\right)^{-\epsilon} \int_0^{\delta_s\sqrt{s_{12}}/2} dE_5 E_5^{-1-2\epsilon} = \left(-\frac{1}{2\epsilon}\right)(\delta_s)^{-2\epsilon}, \tag{A7}$$

and

$$I_A^{jk} = \int_0^\pi \sin^{1-2\epsilon}\theta_1 d\theta_1 \int_0^\pi \sin^{-2\epsilon}\theta_2 d\theta_2 \frac{1}{1-\beta_j\cos\theta_1} \times \frac{1}{1-\beta_k\cos\theta\cos\theta_1 - \beta_k\sin\theta\sin\theta_1\cos\theta_2}. \tag{A8}$$

The way to calculate the integrals I_A^{jk} can be found in the appendix of Ref. [32]. Now we come to the results. It is easy to obtain

$$I^{11} = I^{22} = I^{44} = 0, \tag{A9}$$

and the others are listed below.

(1) I^{1i} with $i = 2, 3, 4$. Write the momenta of the particles as

$$\begin{aligned} p_1 &= E_1(1, \cdots, 1), \\ p_2 &= E_2(1, \cdots, -1), \\ p_3 &= E_3(1, \cdots, \beta\sin\theta_{13}, \beta\cos\theta_{13}), \\ p_4 &= E_4(1, \cdots, -\sin\theta_{13}, -\cos\theta_{13}), \end{aligned} \tag{A10}$$

then we have

$$\begin{aligned} I_A^{12} &= -\frac{\pi}{\epsilon}, \\ I_A^{13} &= \frac{\pi}{1-\beta\cos\theta_{13}}\left\{-\frac{1}{\epsilon} + \ln\frac{(1-\hat{t})^2}{\hat{s}} - \epsilon\left[\ln^2(1-\hat{t}) - \frac{1}{2}\ln^2\hat{s} + 2\mathrm{Li}_2(\hat{t}) - 2\mathrm{Li}_2\left(\frac{\hat{u}}{1-\hat{t}}\right)\right]\right\}, \\ I_A^{14} &= -\frac{2\pi}{(1+\cos\theta_{13})\epsilon}\left(\frac{\hat{u}}{1-\hat{s}}\right)^{-\epsilon}\left[1 + \epsilon^2\mathrm{Li}_2\left(\frac{\hat{t}}{1-\hat{s}}\right)\right], \end{aligned} \tag{A11}$$

which lead to

$$\begin{aligned} I^{12} &= -\frac{2}{\pi} I_E I_A^{12} = -\frac{1}{\epsilon^2}\delta_s^{-2\epsilon}, \\ I^{13} &= -\frac{1-\beta\cos\theta_{13}}{\pi} I_E I_A^{13} \\ &= -\frac{1}{2\epsilon^2}\delta_s^{-2\epsilon}\left\{1 - \epsilon\ln\frac{(1-\hat{t})^2}{\hat{s}} + \epsilon^2\left[\ln^2(1-\hat{t}) - \frac{1}{2}\ln^2\hat{s} + 2\mathrm{Li}_2(\hat{t}) - 2\mathrm{Li}_2\left(\frac{\hat{u}}{1-\hat{t}}\right)\right]\right\}, \\ I^{14} &= -\frac{1+\cos\theta_{13}}{\pi} I_E I_A^{14} \\ &= -\frac{1}{\epsilon^2}\delta_s^{-2\epsilon}\left(\frac{\hat{u}}{1-\hat{s}}\right)^{-\epsilon}\left[1 + \epsilon^2\mathrm{Li}_2\left(\frac{\hat{t}}{1-\hat{s}}\right)\right]. \end{aligned} \tag{A12}$$

(2) I^{2i} with $i = 3, 4$. These two can be directly obtained from I_{1i} with the substitution $\hat{t} \leftrightarrow \hat{u}$.

$$\begin{aligned} I^{23} &= -\frac{1}{2\epsilon^2}\delta_s^{-2\epsilon}\left\{1 - \epsilon\ln\frac{(1-\hat{u})^2}{\hat{s}} + \epsilon^2\left[\ln^2(1-\hat{u}) - \frac{1}{2}\ln^2\hat{s} + 2\mathrm{Li}_2(\hat{u}) - 2\mathrm{Li}_2\left(\frac{\hat{t}}{1-\hat{u}}\right)\right]\right\}, \\ I^{24} &= -\frac{1}{\epsilon^2}\delta_s^{-2\epsilon}\left(\frac{\hat{t}}{1-\hat{s}}\right)^{-\epsilon}\left[1 + \epsilon^2\mathrm{Li}_2\left(\frac{\hat{u}}{1-\hat{s}}\right)\right]. \end{aligned}$$

(3) I^{33} and I^{34}. Write the momenta of the final state particles as

$$p_3 = E_3(1, \cdots, -\beta), \qquad p_4 = E_4(1, \cdots, 1), \tag{A13}$$

then

$$
\begin{aligned}
I_A^{33} &= \frac{2\pi}{1-\beta^2}\left[1+\epsilon\frac{1}{\beta}\ln\hat{s}\right],\\
I_A^{34} &= \frac{\pi}{1+\beta}\left\{-\frac{1}{\epsilon}+\ln\hat{s}-\epsilon\left[\frac{1}{2}\ln^2\hat{s}+2\mathrm{Li}_2(1-\hat{s})\right]\right\},\\
I^{33} &= -\frac{1-\beta^2}{\pi}I_E I_A^{33} = \frac{1}{\epsilon}\delta_s^{-2\epsilon}\left[1+\epsilon\frac{1}{\beta}\ln\hat{s}\right],\\
I^{34} &= -\frac{1+\beta}{\pi}I_E I_A^{34}\\
&= -\frac{1}{2\epsilon^2}\delta_s^{-2\epsilon}\left\{1-\epsilon\ln\hat{s}\right.\\
&\quad\left.+\epsilon^2\left[\frac{1}{2}\ln^2\hat{s}+2\mathrm{Li}_2(1-\hat{s})\right]\right\}. \qquad \text{(A14)}
\end{aligned}
$$

APPENDIX B: COLOR FACTORS

Here we present color factors for all the processes involved. Color indices for particle n are labeled as j_n.

1. LO processes

The color factors listed here for LO processes have been orthogonalized and normalized.

(i) $gg \to \Upsilon[^1S_0^{(8)}]g$, three color factors in total:

$$
\begin{aligned}
&\frac{1}{\sqrt{5}}\,\mathrm{Tr}[T^{j_4}T^{j_2}T^{j_1}T^{j_3}-T^{j_4}T^{j_3}T^{j_1}T^{j_2}],\\
&\frac{1}{\sqrt{5}}\,\mathrm{Tr}[T^{j_4}T^{j_3}T^{j_2}T^{j_1}-T^{j_4}T^{j_1}T^{j_2}T^{j_3}],\\
&\frac{1}{\sqrt{5}}\,\mathrm{Tr}[T^{j_4}T^{j_2}T^{j_3}T^{j_1}-T^{j_4}T^{j_1}T^{j_3}T^{j_2}].
\end{aligned} \qquad \text{(B1)}
$$

(ii) $gg \to \Upsilon[^3S_1^{(8)}]g$, three color factors also:

$$
\begin{aligned}
&\frac{1}{3\sqrt{2}}\,\mathrm{Tr}[(T^{j_4}T^{j_2}T^{j_3}T^{j_1}+T^{j_4}T^{j_1}T^{j_3}T^{j_2})\\
&\quad-(T^{j_4}T^{j_1}T^{j_2}T^{j_3}+T^{j_4}T^{j_3}T^{j_2}T^{j_1})],\\
&\frac{1}{3\sqrt{6}}\,\mathrm{Tr}[(T^{j_4}T^{j_2}T^{j_3}T^{j_1}+T^{j_4}T^{j_1}T^{j_3}T^{j_2})\\
&\quad+(T^{j_4}T^{j_1}T^{j_2}T^{j_3}+T^{j_4}T^{j_3}T^{j_2}T^{j_1})\\
&\quad-2(T^{j_4}T^{j_2}T^{j_1}T^{j_3}+T^{j_4}T^{j_3}T^{j_1}T^{j_2})],\\
&\frac{1}{\sqrt{15}}\,\mathrm{Tr}[(T^{j_4}T^{j_2}T^{j_3}T^{j_1}+T^{j_4}T^{j_1}T^{j_3}T^{j_2})\\
&\quad+(T^{j_4}T^{j_1}T^{j_2}T^{j_3}+T^{j_4}T^{j_3}T^{j_2}T^{j_1})\\
&\quad+(T^{j_4}T^{j_2}T^{j_1}T^{j_3}+T^{j_4}T^{j_3}T^{j_1}T^{j_2})].
\end{aligned} \qquad \text{(B2)}
$$

(iii) $gq \to \Upsilon[^1S_0^{(8)}]q$, only one color factor:

$$
\frac{1}{2\sqrt{15}}[3(T^{j_1}T^{j_3}+T^{j_3}T^{j_1})_{j_4j_2}-\delta_{j_4j_2}\delta_{j_1j_3}]. \qquad \text{(B3)}
$$

(iv) $gq \to \Upsilon[^3S_1^{(8)}]q$, two color factors:

$$
\frac{\sqrt{3}}{4}(T^{j_3}T^{j_1})_{j_4j_2},\quad -\frac{1}{4\sqrt{21}}(8T^{j_1}T^{j_3}+T^{j_3}T^{j_1})_{j_4j_2}. \qquad \text{(B4)}
$$

(v) $q\bar{q} \to \Upsilon^{(8)}g$, almost the same as $gq \to \Upsilon^{(8)}q$.

2. Virtual correction processes

In the amplitude of virtual correction processes, besides the same color factors as in the corresponding LO process, there are extra ones. As we have mentioned before, virtual correction to the cross section is related to virtual amplitude as Eq. (6). Then the terms in proportion to these extra color factors will vanish and do not contribute to the final result as we have orthogonalized the color factors of LO processes. Thus no new color factors in virtual correction processes need to be presented here.

3. Real correction processes

In order to present the color factors of real correction processes in a simplified form, we list here all independent color factors in a certain process. Actually in our calculation, they are orthogonalized and normalized too, which are too complicated to be listed here.

(i) $gg \to \Upsilon[^1S_0^{(8)}]gg$, twelve color factors. The permutations of j_1, j_2, j_3 and j_4 contain 24 terms. Divide them into 12 groups with two terms in each group, and the 12 color factors can be expressed as

$$
\mathrm{Tr}\,[T^{j_5}(T^aT^bT^cT^d+T^dT^cT^bT^a)], \qquad \text{(B5)}
$$

where a, b, c, d are permutations of j_1, j_2, j_3 and j_4.

(ii) $gg \to \Upsilon[^3S_1^{(8)}]gg$, also 12 color factors. They can be expressed as

$$
\mathrm{Tr}\,[T^{j_5}(T^aT^bT^cT^d-T^dT^cT^bT^a)]. \qquad \text{(B6)}
$$

(iii) $gg \to \Upsilon[^1S_0^{(8)}]q\bar{q}$, five independent color factors:

$$
\begin{aligned}
&d^{j_2j_3k}(T^{j_1}T^k)_{j_4j_5},\qquad d^{j_2j_3k}(T^kT^{j_1})_{j_4j_5},\\
&d^{j_1j_3k}(T^{j_2}T^k)_{j_4j_5},\qquad d^{j_1j_3k}(T^kT^{j_2})_{j_4j_5},\\
&6(T^{j_3}T^{j_2}T^{j_1}-T^{j_1}T^{j_2}T^{j_3})_{j_4j_5}+if^{j_1j_2j_3}\delta_{j_4j_5}.
\end{aligned} \qquad \text{(B7)}
$$

(iv) $gg \to \Upsilon[^3S_1^{(8)}]q\bar{q}$, seven independent color factors. One is $d^{j_1j_2j_3}\delta_{j_4j_5}$ while the others can be expressed as

$$(T^a T^b T^c)_{j_4 j_5}, \tag{B8}$$

where a, b, c are permutations of j_1, j_2 and j_3.

(v) $gq \to \Upsilon^{(8)} gq$ and $q\bar{q} \to \Upsilon^{(8)} gg$, similar to $gg \to \Upsilon^{(8)} q\bar{q}$.

(vi) $q\bar{q} \to \Upsilon[^1S_0^{(8)}]q\bar{q}$, two color factors:

$$T^{j_3}_{j_2 j_5}\delta_{j_4 j_1} + T^{j_3}_{j_4 j_1}\delta_{j_2 j_5}, \qquad T^{j_3}_{j_2 j_1}\delta_{j_4 j_5} + T^{j_3}_{j_4 j_5}\delta_{j_2 j_1}. \tag{B9}$$

(vii) $q\bar{q} \to \Upsilon[^3S_1^{(8)}]q\bar{q}$, four color factors:

$$T^{j_3}_{j_2 j_5}\delta_{j_4 j_1}, \quad T^{j_3}_{j_4 j_1}\delta_{j_2 j_5}, \quad T^{j_3}_{j_2 j_1}\delta_{j_4 j_5}, \quad T^{j_3}_{j_4 j_5}\delta_{j_2 j_1}. \tag{B10}$$

(viii) $qq \to \Upsilon^{(8)} qq$, similar to $q\bar{q} \to \Upsilon^{(8)} q\bar{q}$.

(ix) $q\bar{q} \to \Upsilon[^1S_0^{(8)}]q'\bar{q}'$, only one color factor:

$$3(T^{j_3}_{j_2 j_5}\delta_{j_4 j_1} + T^{j_3}_{j_4 j_1}\delta_{j_2 j_5}) - 2(T^{j_3}_{j_2 j_1}\delta_{j_4 j_5} + T^{j_3}_{j_4 j_5}\delta_{j_2 j_1}). \tag{B11}$$

(x) $q\bar{q} \to \Upsilon[^3S_1^{(8)}]q'\bar{q}'$, three color factor:

$$\begin{aligned} &T^{j_3}_{j_2 j_5}\delta_{j_4 j_1} - T^{j_3}_{j_4 j_1}\delta_{j_2 j_5}, \\ &T^{j_3}_{j_2 j_1}\delta_{j_4 j_5} - T^{j_3}_{j_4 j_5}\delta_{j_2 j_1}, \\ &3T^{j_3}_{j_4 j_1}\delta_{j_2 j_5} - T^{j_3}_{j_4 j_5}\delta_{j_2 j_1}. \end{aligned} \tag{B12}$$

(xi) $qq' \to \Upsilon^{(8)} qq'$, similar to $q\bar{q} \to \Upsilon^{(8)} q'\bar{q}'$.

[1] E. Braaten and S. Fleming, Phys. Rev. Lett. **74**, 3327 (1995).
[2] G. T. Bodwin, E. Braaten, and G. P. Lepage, Phys. Rev. D **51**, 1125 (1995).
[3] M. Kramer, Prog. Part. Nucl. Phys. **47**, 141 (2001).
[4] J. P. Lansberg, Int. J. Mod. Phys. A **21**, 3857 (2006).
[5] K. Abe *et al.* (BELLE Collaboration), Phys. Rev. Lett. **88**, 052001 (2002); K. Abe *et al.* (Belle Collaboration), Phys. Rev. Lett. **89**, 142001 (2002); K. Abe *et al.* (Belle Collaboration), Phys. Rev. D **70**, 071102 (2004); P. Pakhlov *et al.* (Belle Collaboration), Phys. Rev. D **79**, 071101 (2009).
[6] B. Aubert *et al.* (*BABAR* Collaboration), Phys. Rev. D **72**, 031101 (2005).
[7] Y. J. Zhang, Y. j. Gao, and K. T. Chao, Phys. Rev. Lett. **96**, 092001 (2006); Y. J. Zhang and K. T. Chao, Phys. Rev. Lett. **98**, 092003 (2007); Y. J. Zhang, Y. Q. Ma, and K. T. Chao, Phys. Rev. D **78**, 054006 (2008); Y. Q. Ma, Y. J. Zhang, and K. T. Chao, Phys. Rev. Lett. **102**, 162002 (2009); B. Gong and J. X. Wang, Phys. Rev. D **77**, 054028 (2008); B. Gong and J. X. Wang, Phys. Rev. Lett. **100**, 181803 (2008); **102**, 162003 (2009); W. L. Sang and Y. Q. Chen, Phys. Rev. D **81**, 034028 (2010); D. Li, Z. G. He, and K. T. Chao, Phys. Rev. D **80**, 114014 (2009); Y. J. Zhang, Y. Q. Ma, K. Wang, and K. T. Chao, Phys. Rev. D **81**, 034015 (2010).
[8] B. Gong and J. X. Wang, Phys. Rev. D **80**, 054015 (2009).
[9] G. T. Bodwin, D. Kang, T. Kim, J. Lee, and C. Yu, AIP Conf. Proc. **892**, 315 (2007); Z. G. He, Y. Fan, and K. T. Chao, Phys. Rev. D **75**, 074011 (2007); G. T. Bodwin, J. Lee, and C. Yu, Phys. Rev. D **77**, 094018 (2008); Z. G. He, Y. Fan, and K. T. Chao, Phys. Rev. D **81**, 054036 (2010); Y. Jia, Phys. Rev. D **82**, 034017 (2010).
[10] S. J. Brodsky and J. P. Lansberg, Phys. Rev. D **81**, 051502 (2010); J. P. Lansberg, Phys. Lett. B **695**, 149 (2011).
[11] Y. Q. Ma, K. Wang, and K. T. Chao, arXiv:1002.3987.
[12] M. Kramer, Nucl. Phys. **B459**, 3 (1996).
[13] P. Artoisenet, J. M. Campbell, F. Maltoni, and F. Tramontano, Phys. Rev. Lett. **102**, 142001 (2009); C. H. Chang, R. Li, and J. X. Wang, Phys. Rev. D **80**, 034020 (2009).
[14] M. Butenschoen and B. A. Kniehl, Phys. Rev. Lett. **104**, 072001 (2010).
[15] R. Li and J. X. Wang, Phys. Lett. B **672**, 51 (2009); J. P. Lansberg, Phys. Lett. B **679**, 340 (2009).
[16] Z. G. He, R. Li, and J. X. Wang, arXiv:0904.1477; Z. G. He, R. Li, and J. X. Wang, Phys. Rev. D **79**, 094003 (2009).
[17] Z. G. He and J. X. Wang, Phys. Rev. D **81**, 054030 (2010).
[18] R. Li, Y. J. Zhang, and K. T. Chao, Phys. Rev. D **80**, 014020 (2009); C. F. Qiao, L. P. Sun, and P. Sun, J. Phys. G **37**, 075019 (2010); P. Ko, C. Yu, and J. Lee, Phys. Rev. D **83**, 054015 (2011); J. High Energy Phys. 01 (2011) 070.
[19] R. Li and J. X. Wang, Phys. Rev. D **82**, 054006 (2010).
[20] A. Abulencia *et al.* (CDF), Phys. Rev. Lett. **99**, 132001 (2007).
[21] V. M. Abazov *et al.* (D0), Phys. Rev. Lett. **101**, 182004 (2008).
[22] E. Braaten and J. Lee, Phys. Rev. D **63**, 071501 (2001).
[23] J. Campbell, F. Maltoni, and F. Tramontano, Phys. Rev. Lett. **98**, 252002 (2007).
[24] B. Gong and J.-X. Wang, Phys. Rev. Lett. **100**, 232001 (2008).
[25] B. Gong and J.-X. Wang, Phys. Rev. D **78**, 074011 (2008).
[26] C.-F. Qiao and J.-X. Wang, Phys. Rev. D **69**, 014015 (2004).
[27] P. Artoisenet, J. P. Lansberg, and F. Maltoni, Phys. Lett. B **653**, 60 (2007).
[28] B. Gong, X. Q. Li, and J.-X. Wang, Phys. Lett. B **673**, 197 (2009).
[29] P. Artoisenet, J. M. Campbell, J. P. Lansberg, F. Maltoni, and F. Tramontano, Phys. Rev. Lett. **101**, 152001 (2008).

[30] P. L. Cho and A. K. Leibovich, Phys. Rev. D **53**, 6203 (1996).
[31] M. Klasen, B. A. Kniehl, L. N. Mihaila, and M. Steinhauser, Nucl. Phys. **B713**, 487 (2005).
[32] B. W. Harris and J. F. Owens, Phys. Rev. D **65**, 094032 (2002).
[33] G. Altarelli, R. K. Ellis, and G. Martinelli, Nucl. Phys. **B157**, 461 (1979).
[34] J. Pumplin *et al.*, J. High Energy Phys. 07 (2002) 012.
[35] K. Nakamura *et al.* (Particle Data Group), J. Phys. G **37**, 075021 (2010).
[36] V. M. Abazov *et al.* (D0), Phys. Rev. Lett. **94**, 232001 (2005).
[37] D. E. Acosta *et al.* (CDF), Phys. Rev. Lett. **88**, 161802 (2002).
[38] E. Braaten, S. Fleming, and A. K. Leibovich, Phys. Rev. D **63**, 094006 (2001).
[39] T. Affolder *et al.* (CDF), Phys. Rev. Lett. **84**, 2094 (2000).
[40] T. Kuhr (for the CDF Collaboration) Proc. Sci., DIS2010 (2010) 159 [arXiv:1011.0161].